

# Synthesis and characterization of $\text{Al}_2\text{O}_3\text{-SiO}_2\text{-MgO}$ nanocomposite prepared by sol–gel process as an efficient catalyst for the Knoevenagel condensation of aldehydes with malononitrile

Mahmood Iranpour Mobarakeh · Ali Saffar-Teluri ·  
S. A. Hassanzadeh Tabrizi

Received: 30 May 2014 / Accepted: 7 July 2014  
© Springer Science+Business Media Dordrecht 2014

**Abstract** The composite of  $\text{Al}_2\text{O}_3\text{-SiO}_2$  and  $\text{Al}_2\text{O}_3\text{-SiO}_2\text{-MgO}$  nanocomposite were synthesized by sol–gel method and FT-IR, XRD, FE-SEM, EDAX, TEM, and BET surface area analysis were used to characterize the as-prepared samples. XRD results show the formation of MgO phase in the nanocomposite. FE-SEM images indicate uniform distribution of MgO nanoparticles in the  $\text{Al}_2\text{O}_3\text{-SiO}_2$  matrix and also amorphous and spherical-like structures for  $\text{Al}_2\text{O}_3\text{-SiO}_2$  and  $\text{Al}_2\text{O}_3\text{-SiO}_2\text{-MgO}$  nanocomposite, respectively. An increase in the surface area of the nanocomposite compared to  $\text{Al}_2\text{O}_3\text{-SiO}_2$  composite is observed with adding MgO. The catalytic activity of  $\text{Al}_2\text{O}_3\text{-SiO}_2\text{-MgO}$  nanocomposite was tested by using them as an efficient base catalyst for the Knoevenagel condensation of different aromatic aldehydes with malononitrile at room temperature. The nanocomposite can be easily separated and reused for several cycles.

**Keywords** Nanocomposite · Sol–gel method · Knoevenagel condensation

## Introduction

The formation of  $\text{C}=\text{C}$  bonds in the organic compounds is one of the most useful reactions in the synthesis of therapeutic drugs [1], natural products [2], herbicides, insecticides, functional polymers [3], and fine chemicals [4]. This bond can be formed by the Knoevenagel condensation. The Knoevenagel reaction is the

---

M. I. Mobarakeh · A. Saffar-Teluri (✉) · S. A. H. Tabrizi  
Faculty of Material Science & Engineering, Najafabad Branch, Islamic Azad University,  
PO Box 85141-43131, Najafabad, Iran  
e-mail: a.saffar.t@iaun.ac.ir

A. Saffar-Teluri  
Department of Chemistry, Faculty of Science, Najafabad Branch, Islamic Azad University,  
PO Box 85141-43131, Najafabad, Iran

condensation of an aromatic aldehyde and a compound containing an active methylene group, which proceeds in the presence of a catalyst. The catalysts are ammonia, organic amines and their salts [5], some Lewis acids, and bases such as  $\text{ZnCl}_2$ ,  $\text{CdI}_2$ , zeolites, hydrotalcite in ionic liquid media, amino-functionalized mesoporous silica, and metal–organic frameworks have also been used as catalysts [6–17]. However, some of these methods are limited by harsh conditions, low yields, long reaction times, and use of toxic solvents.

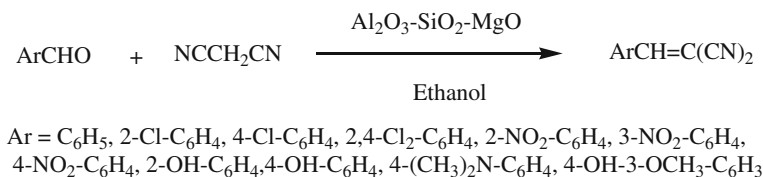
$\text{Al}_2\text{O}_3$ – $\text{SiO}_2$  mixed oxides, or composites of them, as an inorganic support are widely used as catalysts and ceramic materials [18–25]. Clay minerals [18], zeolites [19, 23], mullite [21], and  $\text{SiO}_2$ – $\text{Al}_2\text{O}_3$  catalysts are examples of materials where the existence of Al–O–Si bond structures or  $\text{SiO}_2$ – $\text{Al}_2\text{O}_3$  interfaces controls their final performance for the desired application. The reason for choosing these particular mixed oxides was the properties such as low thermal expansion and conductivity, low dielectric constant, excellent creep resistance, robust chemical and thermal stability, good high temperature strength, and oxidation resistance [24].

Metal oxides have potential applications in water treatment due to their high surface area added to low production and regeneration costs. Among the large family of metal oxides, magnesium oxide (MgO) is an interesting multifunctional and an exceptionally important material used in catalysis [26], toxic-waste remediation, or as an additive in refractory, paint, and superconducting products as well as for fundamental and application studies [27]. It has also been used as bactericides and adsorbents. MgO in particular has shown great promise as a destructive adsorbent for toxic chemical agents [28]. MgO is mainly obtained by the thermal decomposition of magnesium hydroxide or carbonate, sol–gel process, spray pyrolysis, sonochemical synthesis, and hydrothermal reaction [28–31]. The MgO morphology and particle size were found to depend on the preparation conditions such as pH, gelling agent, calcination rate, and temperature.

In the past few years, the synthesis of solid base catalysts has played a prominent role in the field of heterogeneous catalysis. Solid base catalysts have several advantages over homogeneous base catalysts, such as easy recovery of the catalyst, simple product isolation, and recyclability. Thus, the heterogeneous solid base catalysts have been recognized as potential alternatives to homogeneous base catalysts. In an effort to design various solid base catalysts for the synthesis of  $\alpha,\beta$ -unsaturated dicyanide derivatives and in continuation of our interest in the use of heterogeneous catalyst in organic reactions [32–35], herein we report a novel and mild condensation of various aromatic aldehydes with malononitrile reaction for the synthesis of  $\alpha,\beta$ -unsaturated dicyanides using reusable  $\text{Al}_2\text{O}_3$ – $\text{SiO}_2$ –MgO catalyst at room temperature (Scheme 1).

## Experimental

All reagents were purchased from Merck and Aldrich and used without further purification. All products obtained are known compounds and were identified by comparing their physical and spectral data with those reported in the literature.  $^1\text{H}$  NMR spectra were recorded on an Ultra Shield spectrometer (400 MHz) using TMS as



**Scheme 1** Knoevenagel condensation aromatic aldehydes with malononitrile

internal standard. Fourier transform infrared (FT-IR) spectroscopy was performed using a Jasco FT/IR-3600 FT-IR spectrometer. The phase and crystallinity were characterized by using a Philips x'pert X-ray diffractometer with Cu-K<sub>α</sub> radiation in the 2θ range of 10–70°. FE-SEM and EDAX were taken by a SIGMA VP field emission scanning electron microscopy. Specific surface area was carried out using Micrometrics adsorption equipment (BELSORP Instrument, Japan).

### Synthesis of Al<sub>2</sub>O<sub>3</sub>–SiO<sub>2</sub>–MgO nanocomposite

Al<sub>2</sub>O<sub>3</sub>–SiO<sub>2</sub>–MgO nanocomposite with 50 wt% of MgO was synthesized using the sol–gel approach. Firstly, tetraethyl orthosilicate (TEOS) was diluted in ethanol and water. Then the necessary amount of HCl (37 %) was added to the mixture and refluxed at 75 °C for 2 h (TEOS: C<sub>2</sub>H<sub>5</sub>OH: H<sub>2</sub>O: HCl molar ratio was 1:22:13: 7.9 × 10<sup>−4</sup>). Afterwards, magnesium nitrate (Mg(NO<sub>3</sub>)<sub>2</sub>·6H<sub>2</sub>O) and aluminum nitrate (Al(NO<sub>3</sub>)<sub>3</sub>·9H<sub>2</sub>O) dissolved in ethanol was added to the mixture and refluxed at 75 °C for another 2 h. The resulting mixture was aged at room temperature for 24 h and dried in an oven for 24 h at 120 °C. It was then calcined to 500 °C at a heating rate of 8 °C/min and once 500 °C was reached, it was kept at this temperature for 12 h. The nominal content of MgO was 50 wt%, and the corresponding nanocomposite was denoted as ASM50. Also, Al<sub>2</sub>O<sub>3</sub>–SiO<sub>2</sub> composite was synthesized under similar conditions.

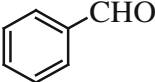
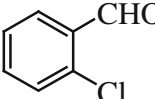
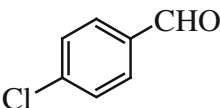
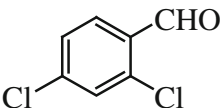
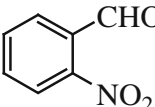
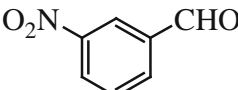
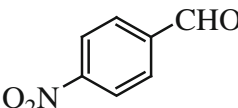
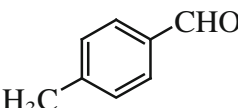
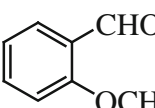
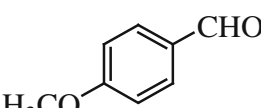
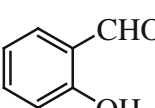
### Synthesis of α,β-unsaturated dicyanides from the condensation reaction of different aromatic aldehydes with malononitrile

In a typical procedure, 1 mmol aromatic aldehyde was mixed with the 1 mmol malononitrile in 5 ml of ethanol taken in a round-bottom flask. Then 20 mg ASM50 was added to it and the reaction mixture was stirred at room temperature for the presented time in Table 1. The progress of the reaction was monitored by TLC. After this reaction mixture was filtered, the solid was washed with the ethanol and dried. The solvent was removed and the obtained solid product residue was crystallized from ethanol.

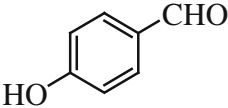
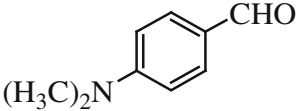
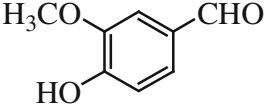
## Results and discussion

Figure 1 presents the FTIR spectrum of ASM50 sample after calcining at 500 °C.

**Table 1** ASM50 nanocomposite catalyzed Knoevenagel condensation

Entry	1	Substrate	Time (min)	Yield (%) <sup>a</sup>	m.p. (°C)	Lit. m.p. (°C) [ref.]
1	a		90	91	81–84	82–85 [36]
2	b		70	90	81–83	80–82 [36]
3	c		60	94	160–162	160 [36]
4	d		50	93	141–142	141–143 [37]
5	e		40	95	136–138	137–138 [37]
6	f		50	93	98–101	100–102 [37]
7	g		20	96	160–163	160–162 [39]
8	h		100	89	131–133	132–133 [36]
9	i		120	90	84–86	84–86 [38]
10	j		140	88	110–112	111–115 [36]
11	k		180	90	163–165	163–164 [40]

**Table 1** continued

Entry	1	Substrate	Time (min)	Yield (%) <sup>a</sup>	m.p. (°C)	Lit. m.p. (°C) [ref.]
12	l		200	87	186–188	187–188 [38]
13	m		150	90	179–182	180–181 [40]
14	n		205	91	135–138	136.5–139 [40]

<sup>a</sup> Isolated yields

In Fig. 1, the absorption peaks  $427$  and  $517\text{ cm}^{-1}$  are attributed to Mg–O vibration, whereas the peaks obtained at  $619$  and  $712\text{ cm}^{-1}$  indicate Al–O bond vibrations. There is also a band at  $898$  and  $1,023\text{ cm}^{-1}$  duo to the Al–O–Al and Si–O–Si bond stretching vibration. The stretching vibration and bending vibration of the O–H group for water appeared at  $3,444$  and  $1,634\text{ cm}^{-1}$ , respectively.

The room-temperature X-ray diffraction (XRD) patterns of  $\text{Al}_2\text{O}_3\text{--SiO}_2$  and ASM50 are presented in Fig. 2a, b, respectively.

The solid  $\text{Al}_2\text{O}_3\text{--SiO}_2$  displays the characteristic spectral profile of an amorphous structure in the  $2\theta = 23^\circ$  for  $\text{Al}_2\text{O}_3\text{--SiO}_2$  (Fig. 2a). Comparison with the spectrum of  $\text{Al}_2\text{O}_3\text{--SiO}_2$ , With adding the MgO content to 50 wt%, two peaks appear in  $2\theta = 43.22^\circ$  and  $62.98^\circ$  (Fig. 2b), which can be indexed to the structure of MgO (JCPDS card No: 78-0430). In order to obtain detailed structure information of the composite, a low-angle XRD pattern of ASM50 is presented in Fig. 3. The composites do not diffract in the  $2\theta$  range of  $1\text{--}10^\circ$ , which indicates that ASM50 has an amorphous matrix.

Figure 4a, b shows the FE-SEM images and EDAX analysis of samples  $\text{Al}_2\text{O}_3\text{--SiO}_2$  and ASM50.

Two types of morphology, uniform (a) and spherical-like (b), can be seen in the FE-SEM images. Surface morphology of the ASM50 sample is different from the  $\text{Al}_2\text{O}_3\text{--SiO}_2$  as would expected due to formation of MgO in nanocomposite. The  $\text{Al}_2\text{O}_3\text{--SiO}_2$  composite has a uniform structure, while adding MgO to the composite causes the formation of homogeneous spherical-like particles. In the FE-SEM image of ASM50, the MgO nanoparticles exist in the nanocomposites with almost uniform distribution.

The EDAX patterns are performed to identify the elemental composition of the nanocomposite. From the corresponding EDAX spectra,  $\text{Al}_2\text{O}_3\text{--SiO}_2$  composite and ASM50 nanocomposite are composed of Al, Si, and O elements (Fig. 4a) and of Al, Si, O, and Mg elements (Fig. 4b), respectively. These results are in good agreement

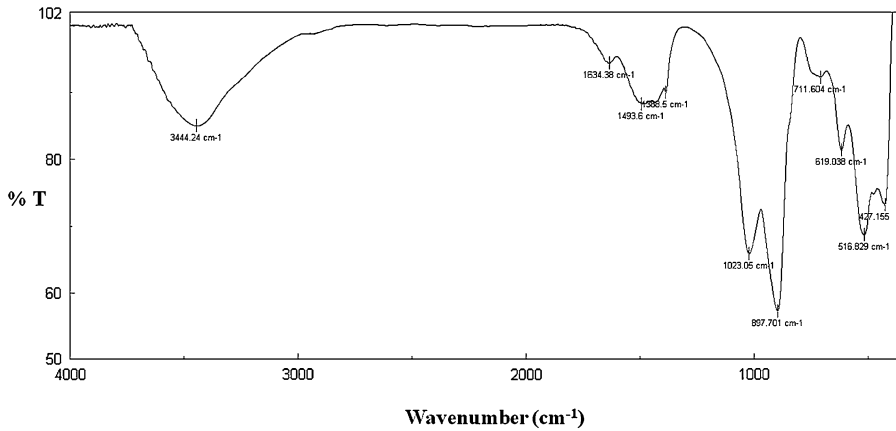


**Fig. 1** The FTIR spectrum of ASM50

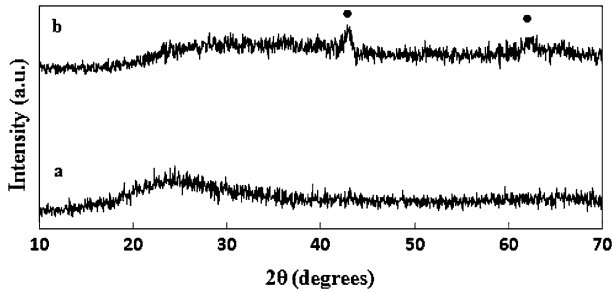
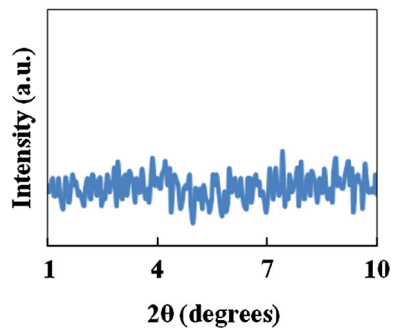


**Fig. 2** XRD patterns of  $\text{Al}_2\text{O}_3\text{--SiO}_2$  (a) and ASM50 (b)

**Fig. 3** Low-angle XRD pattern of ASM50



with the XRD analysis and strongly prove that the MgO is successfully mixed with  $\text{Al}_2\text{O}_3\text{--SiO}_2$  matrix.

In order to obtain the crystallite size of nanocomposite, the TEM image of ASM50 is shown in Fig. 5. Based on Fig. 5, nanoparticle size distribution is

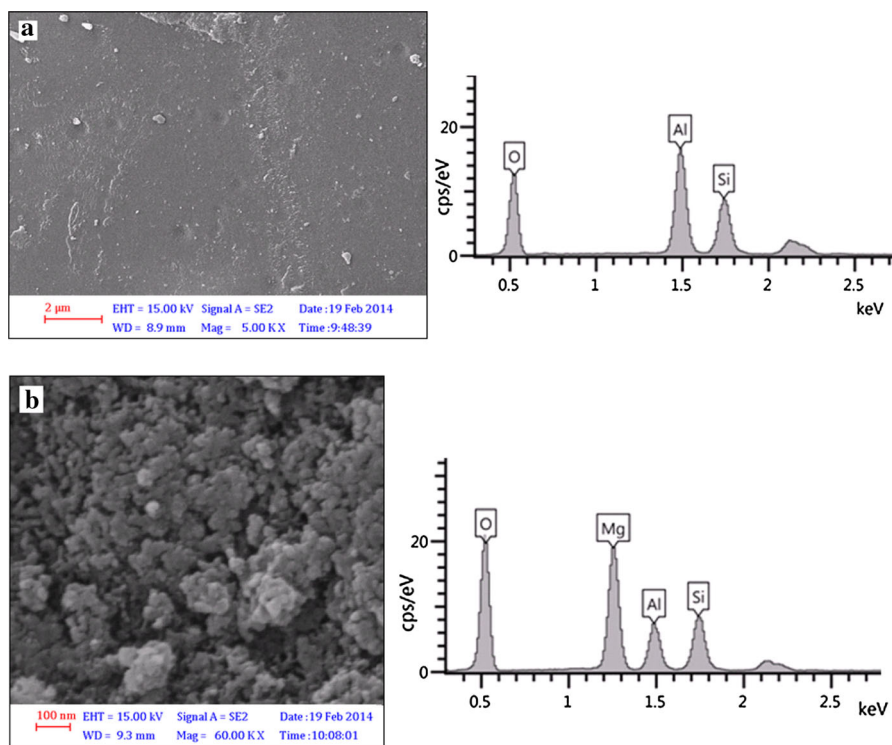


**Fig. 4** FE-SEM images and EDAX analysis of Al<sub>2</sub>O<sub>3</sub>–SiO<sub>2</sub> (a) and ASM50 (b)

continuous between the minimal diameter (about 5 nm) and the maximal diameter (about 90 nm).

The results of BET measurements are presented in Table 2. The Al<sub>2</sub>O<sub>3</sub>–SiO<sub>2</sub> composite has a low BET surface area (63 m<sup>2</sup>/g). With adding MgO, the surface area of the ASM50 nanocomposite was increased (141 m<sup>2</sup>/g).

In order to investigate the catalytic activity of ASM50 nanocomposites, the Knoevenagel condensation between different aromatic aldehydes with malononitrile as active methylene compound was carried out and the results are presented in Table 1. All reactions were completed in 20–205 min duration to produce the corresponding alkenes with 87–96 % yield. Aromatic aldehydes with electron-withdrawing groups (–NO<sub>2</sub>) provided very good yields and the reaction were completed in short times. Also, in the case of electron-donating groups (–OH, –OCH<sub>3</sub>, –CH<sub>3</sub>), reasonably good yields were observed but demanded little more reaction time. In the case of *ortho* and *para* substitutions, the latter gave more yield than the former due to steric hindrance.

Reusability of the catalyst was investigated by carrying out repeated runs on the same batch of the used catalyst. After the completion of the reaction, the catalyst was washed with dichloromethane and acetone, and then dried and recycled. No appreciable change in the activity was observed for five runs (Fig. 6).

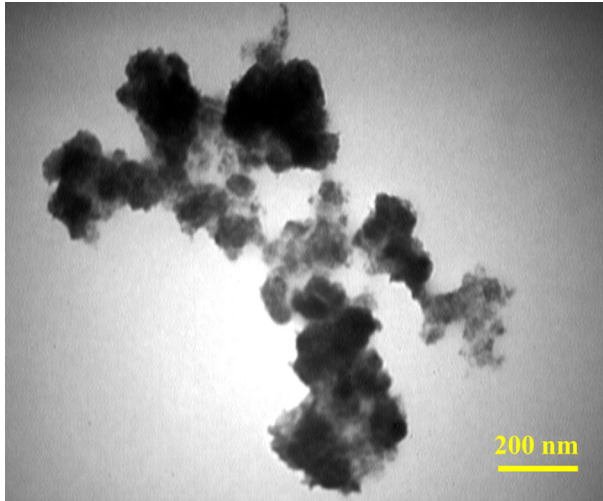


**Fig. 5** TEM image of ASM50

**Table 2** BET measurement results for different nanocomposites

Sample	Surface area (m <sup>2</sup> /g)
Al <sub>2</sub> O <sub>3</sub> –SiO <sub>2</sub>	63
ASM50	141

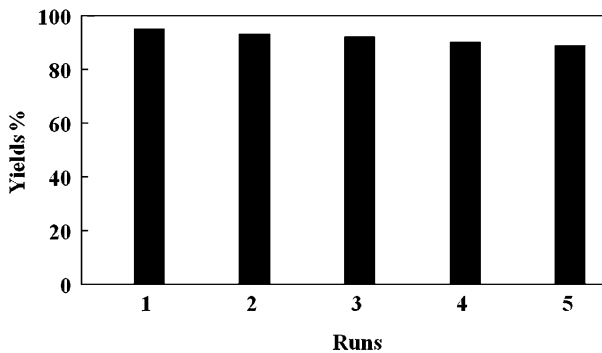


**Fig. 6** Recyclability of ASM50 after fifth cycle

## Conclusions

Based on the above-obtained results, (1) adding MgO to Al<sub>2</sub>O<sub>3</sub>–SiO<sub>2</sub> composite causes an increase in the surface area of the Al<sub>2</sub>O<sub>3</sub>–SiO<sub>2</sub>–MgO nanocomposite, (2) uniform structure of Al<sub>2</sub>O<sub>3</sub>–SiO<sub>2</sub> composite was converted to spherical-like structure by adding MgO in the Al<sub>2</sub>O<sub>3</sub>–SiO<sub>2</sub>–MgO nanocomposite, (3) the reusable Al<sub>2</sub>O<sub>3</sub>–SiO<sub>2</sub>–MgO nanocomposite synthesized through the sol–gel process is an



efficient base catalyst in the Knoevenagel condensation of different aromatic aldehydes with malononitrile for the synthesis of dicyanides with very good yields.

**Acknowledgments** We gratefully acknowledge the financial support from the Research Council of Islamic Azad University of Najafabad Branch.

## References

1. G.A. Kraus, M.E. Krolski, *J. Org. Chem.* **51**, 3347 (1986)
2. L.F. Tietze, *Pure Appl. Chem.* **76**, 1967 (2004)
3. F. Liang, Y. Pu, T. Kurata, J. Kido, H. Nishide, *Polymer* **46**, 3767 (2005)
4. M. Zahouily, M. Salah, B. Bahlaouane, A. Rayadh, A. Houmam, E.A. Hamed, S. Sebti, *Tetrahedron* **60**, 1631 (2004)
5. K. Tanaka, F. Toda, *Chem. Rev.* **100**, 1025 (2000)
6. P.S. Rao, R.V. Venkataratnam, *Tetrahedron Lett.* **32**, 5821 (1991)
7. D. Prajapati, J.S. Sandhu, *J. Chem. Soc. Perkin Trans-I* **1**, 739 (1993)
8. A. Corma, *J. Catal.* **130**, 130 (1991)
9. T.I. Reddy, R.S. Varma, *Tetrahedron Lett.* **38**, 1721 (1997)
10. S.M. Lai, R. Martin-Aranda, K.L. Yeung, *Chem. Commun.* **2**, 218 (2003)
11. F.H. Khan, D. Jyotirmayee, R. Satapathy, S.K. Upadhyay, *Tetrahedron Lett.* **45**, 3055 (2004)
12. G.B.B. Varadwaj, S. Rana, K.M. Parida, *Dalton Trans.* **42**, 5122 (2013)
13. K.M. Parida, S. Mallick, P.C. Sahoo, S.K. Rana, *Appl. Catal. A: Gen.* **381**, 226 (2010)
14. K.M. Parida, D. Rath, *J. Mol. Catal. A: Chem.* **310**, 93 (2009)
15. A. Corma, H. Garcia, *Chem. Rev.* **103**, 4307 (2003)
16. A. Dhakshinamoorthy, M. Opanasenko, J. Čejka, H. Garcia, *Adv. Synth. Catal.* **355**, 247 (2013)
17. A. Dhakshinamoorthy, M. Opanasenko, J. Čejka, H. Garcia, *Catal. Sci. Technol.* **3**, 2509 (2013)
18. S. Wang, *Dyes Pigments* **76**, 714 (2008)
19. M. Sundrarajan, G. Vishnu, K. Joseph, *Dyes Pigments* **75**, 273 (2007)
20. J. Liu, S. Ma, L. Zang, *Appl. Surf. Sci.* **265**, 393 (2013)
21. H. Tajizadegan, M. Jafari, M. Rashidzadeh, A. Saffar-Teluri, *Appl. Surf. Sci.* **276**, 317 (2013)
22. W. Deligeer, Y.W. Gao, S. Asuha, *Appl. Surf. Sci.* **257**, 3524 (2011)
23. M. Anbia, S. Asl-Hariri, S.N. Ashrafzadeh, *Appl. Surf. Sci.* **256**, 3228 (2010)
24. J.P. Chen, S. Wu, *Langmuir* **20**, 2233 (2004)
25. V. Vaccary, *Appl. Clay Sci.* **14**, 161 (1999)
26. M. Arshadi, M. Ghiaci, A. Gil, *Ind. Eng. Chem. Res.* **50**, 13628 (2011)
27. P.J. Sanchez-Soto, J.L. Perez-Rodríguez, I. Sobrados, J. Sanz, *Chem. Mater.* **9**, 677 (1997)
28. M. Arshadi, M. Ghiaci, A.A. Ensafi, H. Karimi-Maleh, S.L. Suib, *J. Mol. Catal. A: Chem.* **338**, 71 (2011)
29. A.A. Ensafi, H. Karimi-Maleh, M. Ghiaci, M. Arshadi, *J. Mater. Chem.* **21**, 15022 (2011)
30. M. Arshadi, M. Ghiaci, *Appl. Catal. A: Gen.* **399**, 75 (2011)
31. M. Arshadi, M. Ghiaci, A. Rahmadian, H. Ghaziaskar, A. Gil, *Appl. Catal. B: Environ.* **119**, 81 (2012)
32. A. Saffar-Teluri, S. Bolouk, *Monatsh. Chem.* **141**, 1113 (2010)
33. A. Saffar-Teluri, *Res. Chem. Intermed.* **39**, 3337 (2013)
34. A. Saffar-Teluri, *Res. Chem. Intermed.* **40**, 1061 (2014)
35. A. Saffar-Teluri, *Res. Chem. Intermed.* **40**, 523 (2014)
36. C. Yue, A. Mao, Y. Wei, M. Lu, *Catal. Commun.* **9**, 1571 (2008)
37. M. Seifi, H. Sheibani, *Catal. Lett.* **126**, 275 (2008)
38. X.S. Wang, Z.S. Zeng, Y.L. Li, D.Q. Shi, S.J. Tu, X.Y. Wei, Z.M. Zong, *Synth. Commun.* **35**, 1915 (2005)
39. S. Mallouk, Kh Bougrin, A. Laghzizilm, R. Benhida, *Molecules* **15**, 813 (2010)
40. B.B. Corson, R.W. Stoughton, *J. Am. Chem. Soc.* **50**, 2825 (1928)